Development of Technique and Determination of Data," *AIChE J.*, **12**, 1147 (1966).

————, "Diffusion and Solution of Gases into Thermally Softened or Molten Polymers: Part II. Relation of Diffusivities and Solubilities with Temperature, Pressure, and Structural Characteristics," *ibid.*, **15**, 106 (1969).

Everett, D. H., and C. T. H. Stoddart, "The Thermodynamics of Hydrocarbon Solutions from G.L.C. Measurements Part I. Solutions in Dinonyl Phthalate," *Trans. Faraday Soc.*, **57**, 746 (1961).

Lichtenthaler, R. N., D. D. Liu, and J. M. Prausnitz, "Polymer-Solvent Interactions from Gas-Liquid Chromatography with Capillary Columns," *Macromolecules*, **7**, 565 (1974).

Lundberg, J. L., M. B. Wilk, and M. J. Huyett, "Estimation of Diffusivities and Solubilities from Sorption Studies," *J. Polymer Sci.*, **57**, 275 (1962).

————, "Sorption Studies Using Automation and Computation," *Ind. Eng. Chem. Fundamentals*, **2**, 37 (1963).

Lyckman, E. W., C. A. Eckert, and J. M. Prausnitz, "Generalized Reference Fugacities for Phase Equilibrium Thermodynamics," *Chem. Eng. Sci.*, **20**, 685 (1965).

Newitt, D. M., and E. W. Weale, "Solution and Diffusion of Gases in Polystyrene at High Pressures," *J. Chem. Soc. (London)*, 1541 (1948).

Newman, R. D., and J. M. Prausnitz, "Polymer-Solvent Interactions from Gas-Liquid Partition Chromatography," *J. Phys. Chem.*, **76**, 1492 (1972).

————, "Polymer-Solvent Interaction from Gas-Liquid Chromatography," *J. Paint Technol.*, **45**, No. 585, 33 (1973).

Stern, S. A., J. T. Mullhaupt, and P. J. Gareis, "The Effect of Pressure on the Permeation of Gases and Vapors through Polyethylene. Usefulness of the Corresponding States Principle," *AIChE J.*, **15**, 64 (1969).

Manuscript received January 30, 1975; revision received September 17, and accepted October 16, 1975.

Experimental Study of the Residence Time Distribution in Plasticating Screw Extruders

DAVID WOLF

and

DON H. WHITE

Department of Chemical Engineering
University of Arizona
Tucson, Arizona 85721

Experimental residence time distribution functions for the liquid and solids conveying processes by a screw conveyer and for the polymer in a plasticating extruder were obtained by using a radioactive tracer technique. A comparison was made between the experimental results and several theoretical models available for melt extrusion and mixing processes.

SCOPE

The objective of this study was to obtain experimental data on the residence time distribution (RTD) of polymers in a plasticating extruder. The results were then compared with theoretical models derived for melt extrusion and other mixing unit operations. RTD functions were also obtained for liquid and solids conveying in screw conveyers. A special technique was developed for that purpose by using radioactive material as the tracer. The experiments were performed employing two methods. By the first method the tracer was preactivated and then injected, while by the second method the tracer was first injected and then samples of the output were activated. The effect of several parameters, such as temperatures of the screw and its rotational speed, were also investigated. The information obtained by the RTD function is of interest for the performance of the extruder, especially when time dependent processes take place in the extruder or in the screw conveying process.

CONCLUSIONS AND SIGNIFICANCE

The plasticating extruder is probably the most widely used unit operation in the polymers industry. The mixing conditions, flow patterns, and residence time distribution (RTD) in a plasticating extruder have significant effects on the product, especially when polymers sensitive to heat are extruded or when good mixing of additives is required. For the use of extruders as polymerization reactors, as it is recently being considered, the knowledge of the residence time distribution is even more important. Therefore, an experimental study on the residence time distribution of the polymer material in a single screw plasticating extruder was made and compared with the limited theory available to date. Additional experiments were made with solids conveying and with liquid conveying by the extruder screw so as to be able to model the plasticating extruder and its various zones as closely as possible.

The experiments for the determination of the RTD were made by using a radioactive tracer, and two different techniques were used for the output analysis. Both techniques were found applicable for the RTD determination in the plasticating extrusion process. The tracer used was a master batch of 1% manganese dioxide in polyethylene which in the first method was irradiated in a nuclear reactor before it was injected into the extruder, whereas in the second method it was injected without being irradiated. The post irradiation method is more time consuming but enables one to test the extruder also in cases where radioactive material cannot be handled at the location of the extruder.

David Wolf is with the Ben Gurion University of the Negev, Beer Sheva, Israel, and Weizmann Institute of Science, Rehovot, Israel.

From the RTD experiments, the mixing conditions and flow patterns in the extruder were deduced. The experimental RTD functions have shown that the solids conveying process is very close to plug flow. In the liquid conveying process, the RTD function can be represented by the theoretical model described by Pinto and Tadmor (1970) for the melt extrusion. The RTD for the plasticating extruder shows little difference from the melt extrusion process. Among the various theoretical models used for comparison with the experimental results, the models derived by Pinto and Tadmor (1970) for the melt extrusion and by Wolf and Resnick (1963) for real systems are quite satisfactory. The effect of some parameters, such as RPM of the screw and screw temperature, on the RTD was also investigated. No significant effect on the RTD was found by changes in the rotational speed of the screw, while some increase in mixing was found by cooling the screw.

The significance of knowing the RTD of the polymer in the extruder is in helping to understand the flow conditions in the extruder and in enabling one to predict the performance of the extruder when the time element is to be considered. The experimental techniques described have the potential of analyzing other types of extruders, poorly performing extruders, the effect of addition of static mixers, or the effect of any other change in the extruder on the RTD, flow, and mixing conditions.

One of the important properties in the performance of an extruder is the residence time distribution of the polymer in the extruder. From the residence time distribution (RTD) functions one can learn about the degree of mixing and the life expectancy of particles in the extruder. The RTD is therefore of importance when the time element is to be considered, such as in the case of overheating where the rate of degradation may be affected or for predicting the applicability of the extruder as a polymerization reactor. Owing to technical difficulties involved in measuring RTD in extruders, experimental results can't be found in the literature. Therefore, a technique has been developed for determination of the RTD by using a radioactive tracer, and this technique was used for determining the RTD in plasticating extruders at various operating conditions.

The experimental and measurement techniques for determining the residence time distribution of the polymer in the extruder are discussed. The experimental results for the various operating conditions of the extruder which were studied are analyzed and compared with the results of the theoretical derivations for melt extruders reported by Pinto and Tadmor (1970), Pinto (1969), and Tadmor and Klein (1970). Existing models for real systems (Levenspiel, 1972; Wolf and Resnick, 1963) are also utilized in order to analyze the mixing and residence time in the extruder needed for the prediction of extruder performance.

The effect of the following parameters on the residence time distribution of the extruder was examined: the rotational speed of the screw, the temperature of the screw, and the effect of the die section. The residence time distribution in the extruder for the conveying of viscous liquid and for the conveying of solid polymer with no extrusion were also checked. Thus, data were obtained to correctly model the extrusion process which, as is well known, has a solids conveying section, a melting section with a mixture of solids and liquid material, and finally a metering zone where only liquid is pumped.

THEORY

The theoretical residence time distribution functions for melt extruders were derived by Pinto and Tadmor (1970) and were used for comparison with the experimental results. The equations which they derived based on parallel plates model and constant channel depth were used. The distribution function $E(t)$ is obtained by solving simultaneously Equations (19) and (27) in Pinto and Tadmor's paper (1970), and the cumulative distribution function $F(t)$ is obtained by solving simultaneously Equations (19) and (30) in that paper. Equations (19), (27), and (30) are reproduced here, respectively:

$$t = \frac{L}{3V_b \sin\theta \cos\theta(1+\phi)} \cdot \frac{3a - 1 + 3\sqrt{1+2a-3a^2}}{a[1-a+\sqrt{1+2a-3a^2}]} \quad (1)$$

$$E(t) = \frac{9}{2} \frac{V_b \sin\theta \cos\theta(1+\phi)}{L} \cdot \frac{a^3\,[a-1-\sqrt{1+2a-3a^2}]^3}{(6a^2-4a-1)\sqrt{1+2a-3a^2}+3a-1} \quad (2)$$

$$F(t) = \frac{1}{2}[3a^2 - 1 + (a-1)\cdot\sqrt{1+2a-3a^2}] \quad (3)$$

where $\phi = 2Q\text{-}WHV_Z$ as obtained from Equation (6) in Pinto and Tadmor's paper. The $E(t)$ function gives the fraction of material which spent between time t and $t + dt$ in the system, while the function $F(t)$ gives the fraction of material which spent the time t or less in the system.

Mixing Models

For the two ideal systems, perfect mixing and plug flow, the following equations are applicable:
for perfect mixing

$$F(t) = 1 - \bar{e}^{t/t} \quad (4a)$$

for plug flow

$$F(t) = 0; \quad t < \bar{t}$$
$$F(t) = 1; \quad t \geq \bar{t} \quad (4b)$$

The conditions in the extruder are neither that of perfect mixing nor of plug flow. Therefore, in addition to the RTD functions derived by Pinto and Tadmor, we will also use the RTD function for laminar flow in a pipe (Pinto, 1969) which, in its normalized form, is

$$F(\theta) = 1 - \left(\frac{1}{2\theta}\right)^2; \quad \theta \geq 0.5 \quad (5)$$

Some real residence time distribution by Levenspiel (1972) and by Wolf and Resnick (1963) were also utilized. Two models suggested by Levenspiel, one being the tanks in series model and the other being the dispersion model, are useful.

The tanks in series model considers the system to be composed of a number of perfectly mixed tanks in series, and the number of tanks are so taken as to fit the $(E\theta)$ curve of the simulated system. The time distribution function in this case is

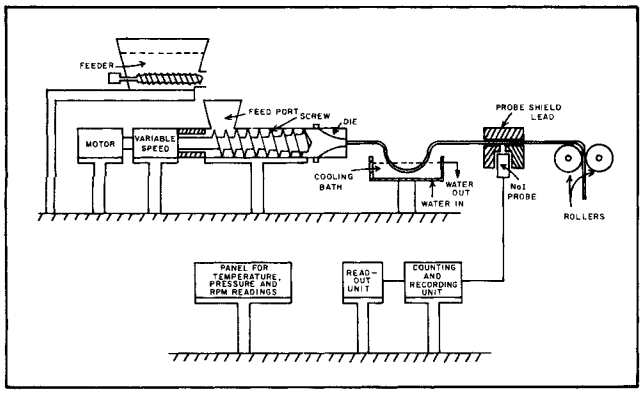

Fig. 1. Schematic view of the experimental setup.

$$E(\theta) = \frac{1}{t\,(n-1)!} \cdot \theta^{(n-1)} \cdot e^{-\theta} \qquad (6)$$

The cumulative distribution function $F(\theta)$ is, as defined, the integral of $E(\theta)$ between 0 and θ for each θ. This model was used by Zinlichem et al. (1973) in the interpretation of their experimental results. This model has as limits the two ideal cases. For $n = 1$ the perfectly mixed vessel case is obtained, and for $n = \infty$ the plug flow condition is simulated. The tanks in series model is a feasible one if one considers the flight dividing the screw in, say, twenty six sections which is the number of turns of the screw. The dispersion model or the axial or longitudinal dispersed plug flow, as it is often called, is also quite a feasible model to be considered here, since much of the flow in the extruder is of the plug flow nature. The concentration distribution function for a tracer impulse and for the nonsymmetrical case is (Levenspiel, 1972)

$$C(\theta) = \frac{1}{2\sqrt{\pi\theta\dfrac{D_e}{uL}}} \cdot e^{-\left[\dfrac{(1-\theta)^2}{4\theta\dfrac{D_e}{uL}}\right]} \qquad (7)$$

where D_e is the eddy diffusivity, u is the axial flow rate, L is the axial length, and D_e/uL is the dispersion number. The inverse of the dispersion number is the Peclet number ($N_{Pe} = uL/D_e$). Since the integration of $C(\theta)$ between zero and infinity is unity, $C(\theta)$ also represents the residence time distribution $E(\theta)$, and the $F(\theta)$ was obtained by integrating the $E(\theta)$ function.

Another model considered is the Wolf and Resnick (1963) model for the real systems, and in its general form it is expressed as follows

$$\begin{aligned} F(\theta) &= 1 - e^{-\eta(\theta-\epsilon/\bar{t})}; \quad \theta \geq \epsilon/\bar{t} \\ F(\theta) &= 0 \qquad\qquad\quad ; \quad 0 < \theta < \epsilon/\bar{t} \end{aligned} \qquad (8)$$

For a combination of plug flow and perfect mixing as we would consider feasible in the extruder, Equation (8) becomes

$$\begin{aligned} F(\theta) &= 1 - e^{-\left(\frac{1}{1-P}\right)(\theta-P)}; \quad \theta \geq P \\ F(\theta) &= 0 \qquad\qquad\qquad\quad ; \quad 0 < \theta < P \end{aligned} \qquad (9)$$

Calculation of Experimental RTD Functions

The experimental results will be compared with all the theoretical RTD functions described here in order to analyze and characterize the flow in the extruder. The experimental distribution functions were calculated by using the data of output concentration vs. time and the following equations (Levenspiel, 1972)

$$E(t) = \frac{C}{\sum_0^\infty C \cdot \Delta t} \qquad (10)$$

$$F(t) = \sum_0^t E(t) \cdot \Delta t = \frac{\sum_0^t C \cdot \Delta t}{\sum_0^\infty C \cdot \Delta t} \qquad (11)$$

$$\bar{t} = \frac{\sum_0^\infty t \cdot C \cdot \Delta t}{\sum_0^\infty C \cdot \Delta t} \qquad (12)$$

Obviously in our case concentration means concentration of radioactive material measured in counts per second. The counts obtained on the recording unit are proportional to the amount of nuclear disintegration of the radioactive material, the shape of the probe and sample, and the distance of the probe from the sample. However, if all physical conditions are kept constant, the difference in the counts from sample to sample is due only to the concentration of the radioactive material in the sample. Since it is common to plot the distribution function in a normalized form and against normalized time, we shall use the following normalized functions:

$$F(\theta) = F(t) = \frac{C(t)}{C(0)} \qquad (13)$$

$$E(\theta) = \bar{t}\,E(t) \qquad (14)$$

and

$$\theta = t/\bar{t} \qquad (15)$$

The mean residence time $\bar{t}$ can also be obtained from the physical conditions

$$\bar{t} = \frac{V}{Q} = \frac{\text{volume or holdup}}{\text{flow rate}} \qquad (16)$$

In a recent work by Tadmor (1973), he assumes that in the solids conveying zone there is complete plug flow. This assumption was also tested in our experimental work.

Correction for the Tapered Channel Depth

Equations (1), (2), and (3) are valid for the constant channel depth. A correction factor for the tapered channel depth as is commonly the case in industrial extruders, and which also was the case in our experiments, was derived. This derivation assumes that the flow remains laminar all along the channel, even though the velocity increases owing to the decrease in channel depth. The mean residence time of a particle entering an extruder with constant channel depth is the ratio between the volume and the flow rate; that is

$$\bar{t} = HLW/Q \qquad (17)$$

For the tapered channel with a linear drop in depth, the mean residence time is

$$\bar{t}_t = \left(hLW + \frac{(H-h)\,LW}{2}\right) \Big/ Q \qquad (18)$$

The correction factor between t_t and t_c is therefore

$$\frac{t_t}{t_c} = \frac{hLW + \dfrac{(H-h)}{2} LW/Q}{HLW/Q} \qquad (19)$$

which, after rearrangement, gives

$$\frac{t_t}{t_c} = \frac{H + h}{2H} = A_w \tag{20}$$

The ratio $H + h/2H$ is the correction factor A_w for the mean residence time in the extruder, and owing to the assumption of laminar flow, this correction factor is valid all along the channel for all values of t calculated from Equation (1). From Equation (16), one can see that when h is equal to H, the A_w factor is one as expected. Also, as h becomes less than H, the A_w factor decreases, thus reducing the mean residence time in the extruder. This is also expected owing to the increase in flow velocity along the screw as the width of the channel is reduced.

EXPERIMENTAL SETUP

For all experiments, a Prodex extruder was used with a screw of 44.2 mm in diameter and 24/1 L/D ratio. The feed section of the screw has nine turns with a constant channel depth of 7.5 mm, the transition or compression section has seven turns with a channel depth decreasing linearly from 7.5 to 1.9 mm, and the metering or melt section has ten turns with a constant channel depth of 1.9 mm. The volume of the channel of the screw was measured by water displacement and found to be 530 cm^3. Excluding the feeding section of the screw in the hopper, the volume of the channel of the screw covered by the barrel is 475 cm^3.

The variable speed unit in the range of 0 to 200 rev./min. was attached to the extruder, and the screw speed could therefore be changed to the desired revoltions per minute. More details on the extruder can be found elsewhere (Felix, 1975; Schott, 1971; White and Schott, 1971). A schematic view of the experimental setup is shown here on Figure 1. All extrusion experiments were made with low density polyethylene pellets as extrudate material. The output from the screw was in the form of a strip of polyethylene.

The experiments on solids conveying were made with reground polyethylene which passed a 7 mesh screen.

Experiments were also made on liquid conveying and the material used was PC-312 standard polyester resin of InMont Corporation.

Tracer Preparation and Detection

As a tracer, manganese dioxide was used in the form of a mixture of polyethylene and manganese dioxide which contained around 1.0% manganese oxide in polyethylene. This master batch was prepared by passing through the extruder 800 g of polyethylene and 8 g of manganese dioxide. The extruded polyethylene was then ground again and well mixed. This ensured a fairly uniform master batch for the trace experiment. The uniformity was not important for the experiment itself but rather to be able to know the irradiation for a desired activity.

The reasons for choosing this particular tracer were its reasonable radiation energy level for detection purposes and its relatively low half-life which avoids longtime radiation pollution problems. The half-life for the γ emitting Mn^{56} isotope is 2.576 hr. (Weast, 1973). The Mn^{56} is obtained by radiation of the stable isotope Mn^{56} in a nuclear reactor. The reaction is

$$Mn^{55} \xrightarrow{(n,\gamma)} Mn^{56} \tag{21}$$

The radiation time is a function of the neutron flux available, the activity required, and the amount of manganese dioxide in the indicated sample. Exact calculations of the activity obtained by irradiation can be found in the book of Chase and Rabinowitz (1962), and some details of calculation are given in the next section. Our trace sample was irradiated in the University of Arizona nuclear reactor with a neutron flux of 10^{12} neutron/cm^2 s. The decisions on the concentration of manganese dioxide in the master batch and the amount of activity were made so as to best satisfy the condition of high signal-to-noise ratio and small amounts of tracer, in order to have a true Dirac pulse, and a low level of radioactivity, in order to reduce radioactive hazards.

The detection of the γ rays emitted by the radioactive tracer was made with a sodium iodide probe 25.4 mm in diameter. The signal from the probe was sent to a recording unit of the Technical Measurement Corporation, where the readings were recorded every second and stored for later retrieval in the form of a strip chart and paper tape. The information on the tape was then transferred to IBM cards which in turn were used for the RTD function calculations.

The background reading of the probe was reduced as much as possible by shielding the probe with lead, first by inserting the probe tip in a lead brick and then by covering all the probe by a sheet of lead. In order to avoid a change in the background due to the accumulated extruded material with its tracer content, the material was carried away from the probe immediately after it passed through the probe.

Calculation of the Isotope Radioactivity

The intensity of the radioactivity of the radioisotope in the sample is a function of radiation time, the time that elapsed since it has been taken out of the reactor and some other parameters, as expressed by

$$I_A = \frac{N\sigma\phi aW}{3.7 \times 10^7 M}\left(1 - e^{-0.693\frac{t_i}{t_{1/2}}}\right)\left(e^{-0.693\frac{t_c}{t_{1/2}}}\right) \tag{22}$$

where $t_{1/2}$ is the half-life of the radioisotope.

Since disintegrations start as the radioisotope is being produced, a saturation condition is eventually obtained where the amount of radioisotope produced equals the amount which disappears by decay. At $t_{1/2}$ the sample reaches 50% of the saturation value. For all practical purposes, saturation is obtained after several half-lives.

Effect of Decay on Experimental Results

Owing to the relatively short half-life of the Mn^{56} isotope, the effect of the decay on the true measurement had to be taken into account. During the 16 min. that the experiments usually ran, the counts reduced by 6%. Therefore, every count was corrected for the time by using the following equation:

$$\frac{C}{C_o} = e^{-\lambda t} \tag{23}$$

Note that this correction factor is the same as the last factor in the equation for the intensity of radioactivity I_A, Equation (22).

EXPERIMENTAL PROCEDURE

The experimental procedure for the determination of the residence time distribution functions involves an impulse stimulus of tracer in the feed stream. This is also known as a Dirac pulse or a delta function in the input. In order to have a true impulse function, special injectors were used. Note that the injection time was instantaneous. After the extruder was at steady state with regard to flow rates, pressure, and temperature conditions, a sample of the tracer was added very quickly into the feed stream, and the time of injection was recorded. For the extrusion

Table 1. Experimental Results for the Conveying of Liquids

Sample No.	Accumulation time, s	No. of counts/20 s Exp. 1	Exp. 2
1	0-10	0	0
2	10-20	0	0
3	20-30	0	0
4	30-40	0	0
5	40-50	0	0
6	50-60	0	0
7	60-70	0	0
8	70-80	0	0
9	80-90	0	0
10	90-100	0	0
11	100-110	16	30
12	110-120	763	1 181
13	120-130	1 094	1 095
14	130-140	421	476
15	140-150	258	271
16	150-160	162	167
17	160-170	109	122
18	170-180	77	92
19	180-190	64	72
20	190-200	53	57
21	200-210	45	49
22	210-220	37	49
23	220-230	35	38
24	230-240	29	29
25	240-250	25	29
26	250-260	26	27
27	260-270	21	28
28	270-280	21	24
29	280-290	20	17
30	290-300	17	22
31	300-310	17	18
32	310-320	15	14
33	320-330	14	14
34	330-340	14	8
35	340-350	14	12
36	350-360	10	10
37	360-370	11	9
38	370-380	10	9
39	380-390	11	11
40	390-400	9	7
41	400-410	12	10
42	410-420	8	6
43	420-430	8	8
44	430-440	8	4
45	440-450	10	7
46	450-460	6	6
47	460-470	1	4
48	470-480	3	10
49	480-490	6	6
50	490-500	1	6
51	500-510	0	7
52	510-520	0	2
53	520-530	0	3
54	530-540	0	3
55	540-550	0	1
56	550-560	0	2
57	560-570	0	0
58	570-580	0	0
59	580-590	0	0
60	590-600	0	0

experiments with activated tracer, the output was continuously monitored, and the measurements of the activity were taken continuously as the plastic strip leaving the extruder passed underneath the sodium iodide probe. After 1 024 s, the experiment was discontinued, and the counting rates which were registered every second in the memory channel were then transferred to IBM cards. These were then used in the calculations of the residence

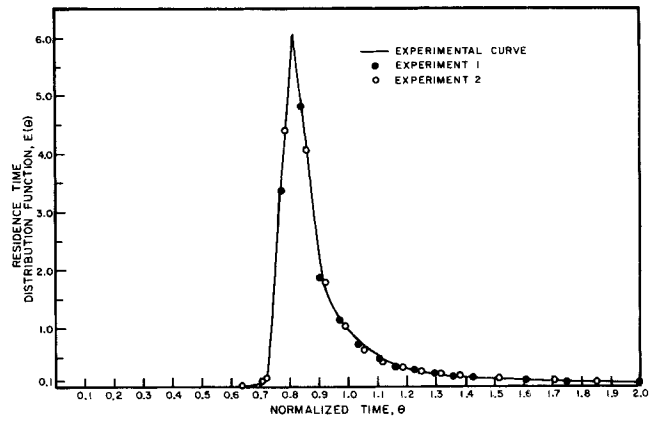

Fig. 2. $E(\theta)$ distribution function for the liquid conveying process.

time distribution functions and the mean residence times. The delay in the reading of the output signal, due to the time it takes the strip to pass the distance between the die outlet and the probe, was measured. A correction of the effect of decay on the measurements was also made in each experiment.

The activation analysis experiments were made with the samples taken from the collected polyethylene strips after the radioactivity had essentially completely decayed and then compared with the normal experimental results, that is, where the tracer was added in the radioactive form.

For the solid conveying experiment, the die section was removed from the extruder, and the solid output was collected in batches at the exit of the extruder and analyzed for its radioactive material content. Neither the barrel nor the screw were heated in this case.

The experiments in the liquid conveying process were also made without the die section and without heating, and the liquid output was also collected in batches for further radiation analysis. The tracer in this case was a master batch of polyester and 1% manganese dioxide. The manganese dioxide which is a fine powder remains in suspension in the polymer for many days.

EXPERIMENTAL RESULTS AND ANALYSES

The experimental results reported in this work will be first for the liquid conveying process, then for the solids conveying process, and then for the plasticating extrusion. This order of presentation was chosen since theoretical RTD functions were derived only for the liquid conveying process as mentioned above, and this aspect should be analyzed first. The solids conveying process was considered next since the assumption of the assumed plug flow condition should be tested. The experimental RTD function for a plasticating extruder is then reported along with the effects of some parameters on these functions.

RTD for Liquid Conveying

The experiment for determining the RTD for liquid conveying by the extruder was done in order to test the theoretical RTD functions derived by Pinto and Tadmor (1970), who derived their equations for the melt extruder. Two experiments were made, and in both cases the rotational speed of the screw was 43 rev./min., and neither the barrel nor the screw was heated. The flow rates Q were in both cases 230 g/min. The injection of the tracer was made with the aid of a syringe made of polyethylene, and the irradiation was made on the syringe directly. The amount of tracer injected was approximately 3 cm^3.

These experiments were made with the original die section removed and replaced by a die plate. After the injection of the tracer, all the output was collected in sixty

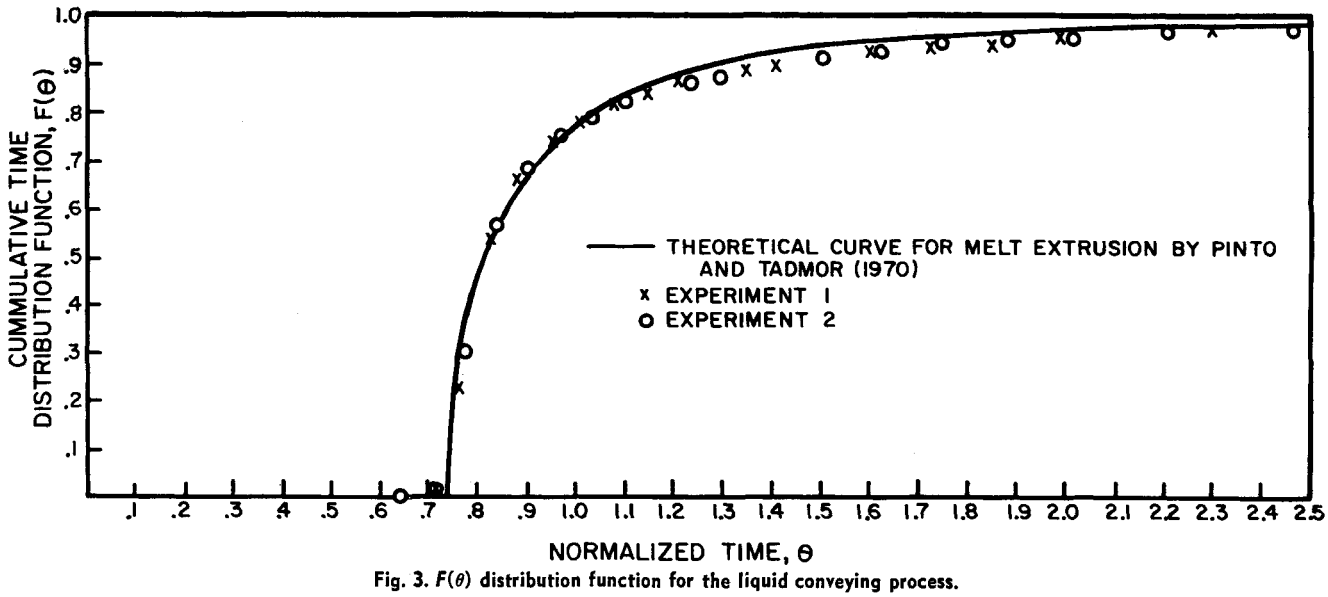

Fig. 3. $F(\theta)$ distribution function for the liquid conveying process.

polyethylene cups for a period of 600 s. Thus, each cup had accumulated material of a 10 sec period. Each sample was then taken for radiation counting, and each counting was for a period of 20 s. The counts per 20 s, after forty-six counts were subtracted for the background, are summarized for both experiments in Table 1. The calculated $E(\theta)$ and $F(\theta)$ functions for both experiments are shown on Figures 2 and 3. One can see on these figures that the results of the same two experiments are very reproducible. Also, one can see on Figure 3 that the experimental results are in very good agreement with the theoretical $F(\theta)$ function derived by Pinto and Tadmor. One should also emphasize that no effect of viscosity on the $F(\theta)$ function is to be expected as long as laminar flow exists.

RTD in the Solids Conveying Process

This experiment, in which the extruder was used as a solids conveyer only, was made with the die removed from the extruder and with no heating of the barrel or the screw. The steady state operating condition for the rotational speed of the screw was 60 rev./min. for a flow rate of 0.8 g/s and a holdup of 35.5 g of the polyethylene regrind. The amount of tracer injected was approximately 1.5 g. After the tracer was injected, the output of material was continuously collected in batches so that each batch consisted of an accumulation of material obtained in 5 s. This was the lowest time possible for sampling. Each batch of material was then tested for the radioactive activity for 20 s. The counts obtained were recorded after the background of the counts were subtracted. The experimental results are summarized in Table 2, and the $E(\theta)$ and $F(\theta)$ functions are shown on Figures 4 and 5. These results were verified by an additional experiment where the same results were obtained. The theoretical curves, with complete plug flow assumed, are also shown on these figures. The analysis of these figures shows that the conveying process is not a complete plug flow, although quite close to it.

RTD in the Plasticating Extrusion Process

In the plasticating extrusion experiment, polyethylene was extruded to form a strip of plastic. When steady state (constant temperatures, pressures, and output flow rate) was reached, we injected the radioactive tracer and started the continuous counting of the radioactivity of the output strip. The counts were accumulated every second, and the number was stored in the memory of the counting

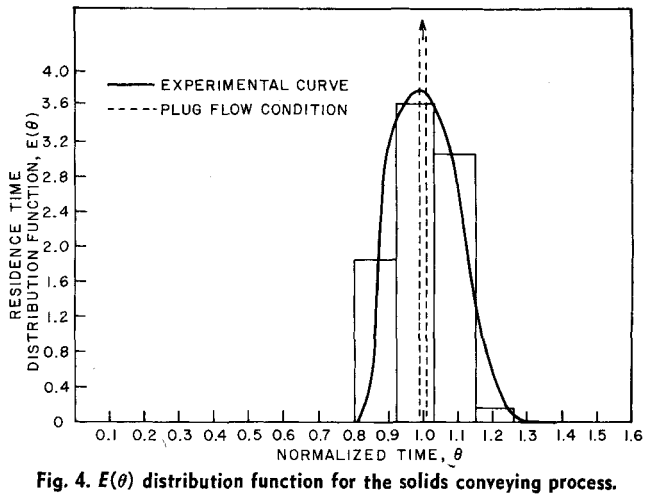

Fig. 4. $E(\theta)$ distribution function for the solids conveying process.

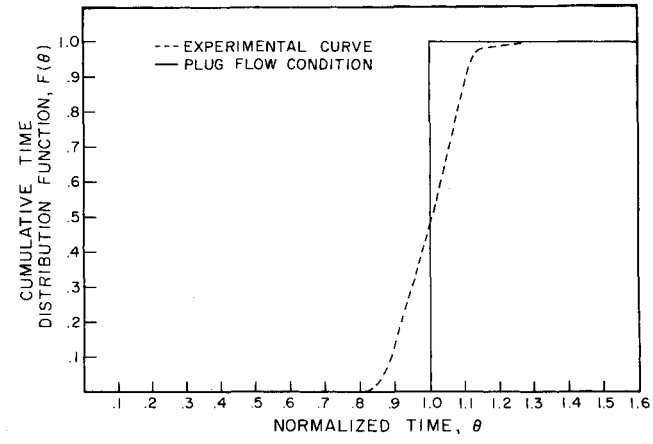

Fig. 5. $F(\theta)$ distribution function for the solids conveying process.

system. At the end of the experiment, the data were used for the $E(\theta)$ and $F(\theta)$ calculations. The operational conditions of a typical experiment are given in Table 3, and the $E(\theta)$ and $F(\theta)$ functions are given in Figures 6 and 7. A comparison between the experimental results and the different theoretical models can be seen on Figures 7, 8, 9, and 10. Analyzing Figures 7, 8, and 9, one can see that the Pinto and Tadmor model developed for the melt extrusion is a better representation for the plasticating extruder

TABLE 2. TYPICAL EXPERIMENTAL RESULTS FOR RTD IN THE SOLIDS CONVEYING PROCESS

No. of sample	t accumulated time, s	c counts/s	$c \cdot \Delta t$	$c \cdot t^*$	θ	$E(t) = \frac{c}{\Sigma c \Delta t}$	$E(t)\Delta t$	$E(\theta) = \bar{t}E(t)$	$F(t) = F(\theta)$
1	0-5	0	0	0	0.115	0	0	0	0
2	5-10	0	0	0	0.230	0	0	0	0
3	10-15	0	0	0	0.345	0	0	0	0
4	15-20	0	0	0	0.460	0	0	0	0
5	20-25	0	0	0	0.576	0	0	0	0
6	25-30	0	0	0	0.691	0	0	0	0
7	30-35	0	0	0	0.806	0	0	0	0
8	35-40	17 460	87 300	654 750	0.921	0.04252	0.2126	1.845	0.2126
9	40-45	34 120	170 600	1 450 100	1.036	0.08310	0.4155	3.606	0.6281
10	45-50	29 000	145 000	1 377 500	1.152	0.07063	0.3531	3.065	0.9812
11	50-55	1 270	6 350	66 675	1.267	0.00309	0.0155	0.134	0.9967
12	55-60	80	400	4 600	1.382	0.00019	0.0009	0.008	0.9976
13	60-65	20	100	1 250	1.497	0.00005	0.0002	0 002	0.9978
14	65-70	30	150	2 025	1.612	0.00007	0.0004	0.003	0.9982
15	70-75	20	100	1 450	1.728	0.00005	0.0002	0.002	0.9984
16	75-80	55	275	4 262	1.843	0.00013	0.0006	0.005	0.9990
17	80-85	10	50	825	1.958	0.00002	0.0001	0.001	0.9991
18	85-90	15	75	1 312	2.073	0.00004	0.0002	0.002	0.9993
19	90-95	5	25	462	2.188	0 00001	0.0000	0.001	0.9993
20	95-100	15	75	1 462	2.304	0.00004	0.0002	0.002	0.9995
21	100-105	5	25	512	2.419	0.00001	0 0000	0.001	
22	105-110	0	0	0	2.534	0.00000	0.0000	0.000	
23	110-115	5	25	562	2.649	0.00001	0.0000	0.001	
24	115-120	0	0	0	2.764	0.00000	0 0000	0.000	
25	120-125	0	0	0	2.880	0.00000	0.0000	0.000	1.0000
		$\Sigma = 82\,110$	$\Sigma = 410\,550$						

$$\bar{t} = \frac{\Sigma t \cdot c}{\Sigma c} = 43.4\ s \text{ and } \bar{t} = \frac{V}{Q} = \frac{35}{48} = 43.7\ s.$$

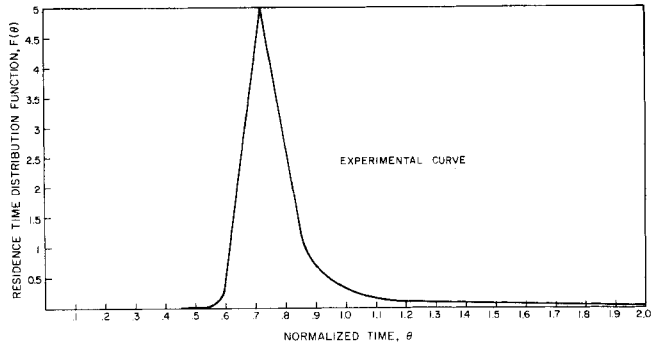

Fig. 6. Typical experimental $E(\theta)$ distribution function for the extrusion processs.

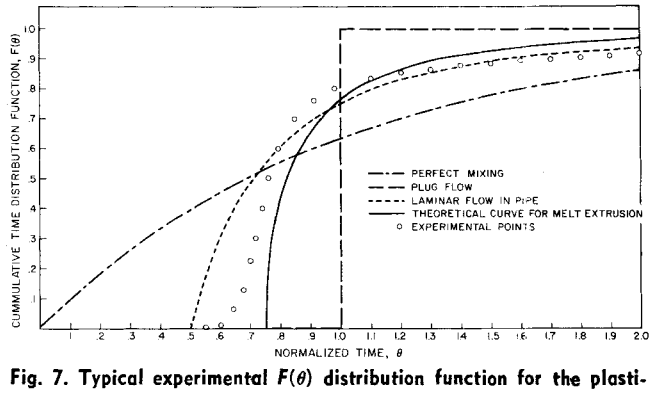

Fig. 7. Typical experimental $F(\theta)$ distribution function for the plasticating extrusion process compared to some theoretical functions.

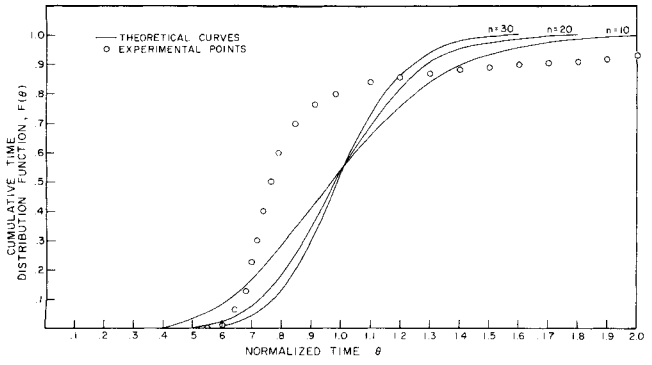

Fig. 8. Typical experimental $F(\theta)$ distribution function for the plasticating extrusion process compared to the tanks in series model.

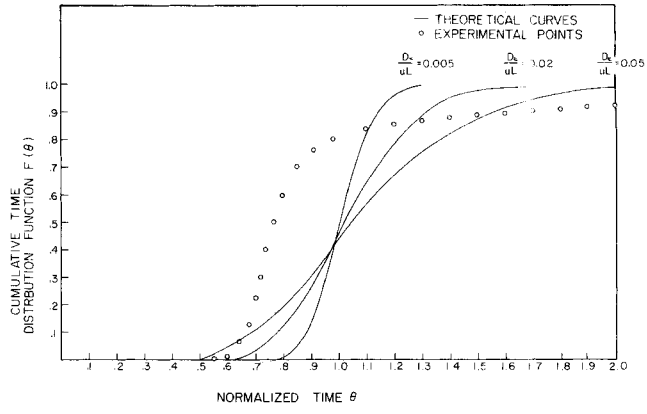

Fig. 9. Typical experimental $F(\theta)$ distribution function for the plasticating extrusion process compared to the dispersion model.

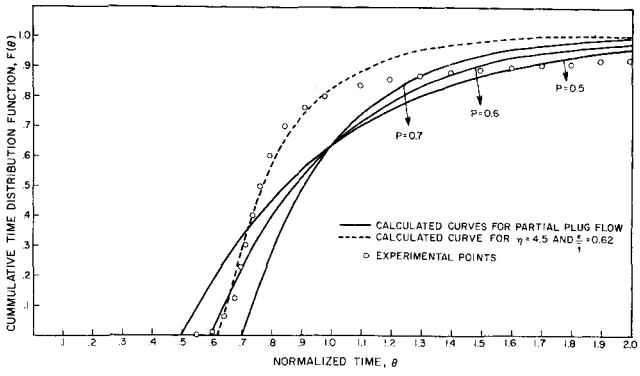

Fig. 10. Typical experimental $F(\theta)$ distribution function for the plasticating extrusion process compared with the Wolf and Resnick model.

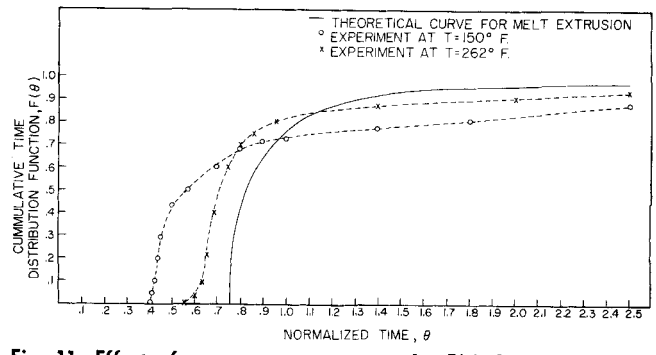

Fig. 11. Effect of screw temperature on the $F(\theta)$ function for the plasticating extrusion process.

than the various flow conditions represented on these figures, such as perfect mixing, plug flow, laminar flow in a pipe, the tanks in series model, and the dispersion model. On Figure 10 one can see that partial plug flow and partial perfect mixing are also not good representations of the RTD in the extruder, and that the Wolf and Resnick approximation model with $\eta = 4.5$ and $\epsilon/\bar{t} = 0.62$ is a better representation of the RTD in the extruder, except for the tail section. However, the tail behavior is not well represented in any model, and it deserves a special investigation. The long tail in the extrusion case was also found by Todd (1974) for twin screw extruders, and this is probably due to effects, such as adhesion, small dead spaces, and low backmixing, which have only secondary effects on the residence time distribution.

Effect of Screw Temperature

Two experiments were made in order to check the effect of screw temperature on the residence time. The temperature of the screw was controlled by passing a stream of oil through the screw of the extruder. In one experiment, the input oil temperature was 65°C and in the other 128°C. All other experimental conditions are given in Table 3. The $F(\theta)$ functions obtained are given on Figure 11, and they show an increase in the mixing as the screw temperature is decreased. The reason for this effect could be the increased viscosity gradient on the melt between the root of the screw and the barrel surface.

Effect of Rotational Speed of the Screw

Five experiments were made in order to test the effect of revolutions per minute of the screw on the RTD. The rotational speeds were 36, 42, 60, 83, and 101 rev./min.

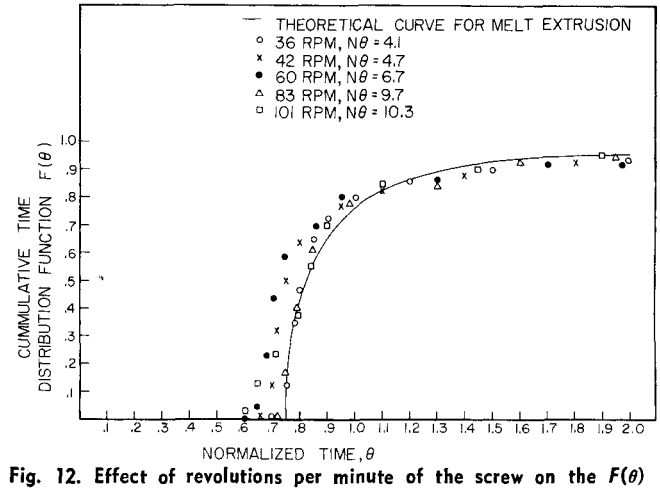

Fig. 12. Effect of revolutions per minute of the screw on the $F(\theta)$ function for the plasticating extrusion process.

The operating conditions are given in Table 3. No significant effect of revolutions per minute was found on the RTD as can be seen on Figure 12.

RTD by Activation of Samples

In order to avoid the use of radioactive material at the location of the extruder itself, the method of activating samples of polymer product after an experimental extruder run was investigated. The reason for considering this method of analysis is the fact that there are cases where radioactive material cannot be used for some reason, for example, owing to lack of technical facilities at the equipment location. Therefore, the addition of the tracer in a nonactivated form would simplify the problem. The sam-

TABLE 3. OPERATIONAL CONDITIONS FOR THE EXTRUSION EXPERIMENTS

Operational conditions	Typical experiment	Effect of screw temperature		Effect of rev./min.				
Rev./min.	43	35	35	36	42	60	83	101
P_1, N/m² × 10⁶	8.2	13.7	12.9	8.0	9.2	10.5	12.2	16.0
P_2, N/m² × 10⁶	15.9	16.7	15.7	14.3	15.0	17.1	18.1	22.0
P_3, N/m² × 10⁶	10.8	13.5	13.0	11.0	12.0	14.6	16.4	18.1
T_1, C°	161	145	156	142	141	140	141	142
T_2, C°	181	166	164	172	171	170	170	171
T_3, C°	182	144	141	193	192	192	191	192
T_4, C°	178	160	162	180	181	181	180	182
T_5, C°	178	169	171	156	155	154	155	156
T_6, C°	179	174	171	189	189	189	189	190
T_7, C°	204	200	200	204	201	206	201	204
T_8, C°	26	26	26	26	27	26	27	26
T_9, C°	—	128	65	—	—	—	—	—
Q, g/s	2.33	2.16	2.42	2.20	2.45	3.63	5.20	6.38

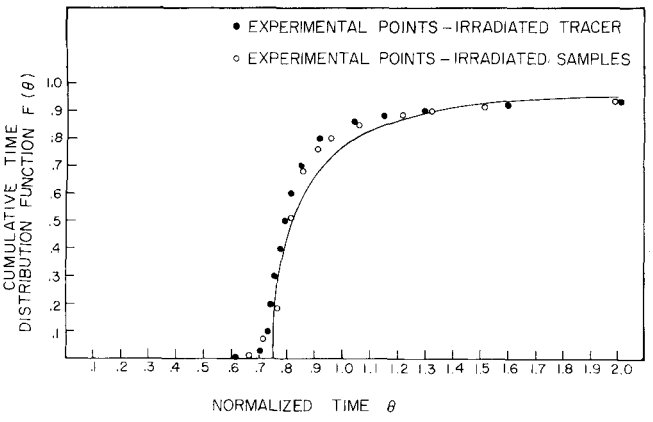

Fig. 13. Comparisin between experimental $F(\theta)$ distribution functions obtained by injecting an activated tracer and by irradiating samples from the output.

ples to be tested are then activated in a nuclear laboratory where all the necessary equipment and safety conditions are available.

First, a normal experiment was done with an activated sample used as a tracer. This experiment was conducted at 43 rev./min. The flow rate was 2.2 g/s, and the length of the strip was 48.5 mm/s. The $F(\theta)$ function of this experiment is shown on Figure 13. The output material from this experiment which was 5.83 m of polyethylene strip was collected for further experimentation. After 48 hr., the strip of material was again analyzed for its radioactivity, and, as expected, the output signal showed that all the radioactivity had decayed. Finally, samples were taken from the strip of polyethylene at intervals of 50 cm, thus accumulating 117 samples. Each sample was a circular disk of 22.5 mm in diameter. These button types of samples were then taken to the nuclear reactor for irradiation. The irradiation time was 600 s, and the irradiated samples were then analyzed, each sample for 20 s. The time after the radiation was recorded along with the counts obtained. The counts obtained were corrected for the height of the sample in the tube and for time of measurement after irradiation. The efficiency of the flux in the reactor as a function of the height was found empirically to be

$$\eta = -0.22\,x + 100 \qquad (24)$$

As one expected, the results were identical to those obtained with the first experimental procedure. From these data the $F(\theta)$ function was calculated, and the result is also shown on Figure 13.

If the irradiated sample includes, in addition to manganese, some other material which is becoming radioactive, one can still use this method of analysis, but one must carry out a spectrum analysis for the γ rays and take into account only the energies obtained from the tracer, in our case manganese.

A second method would be to use a material like Dysprosium which also has a relatively short half-life of 2.3 hr. but has a very high cross section for neutron absorption and therefore needs low power for irradiation. Thus, only the tracer would be activated and not the other material in the sample.

CONCLUSIONS

Experimental data on RTD functions in screw conveyers and plasticating extruders were obtained. A clearer understanding of the mixing conditions for a single screw operating as a solids and liquid conveyer or in a plasticating extruder can also be seen from this study. A considerable amount of plug flow prevails with relatively little apparent mixing. The solids conveying is very close to plug flow, whereas for liquid conveying and for plasticating extrusions between 60 and 70% plug flow was obtained. It is especially interesting to note that the plasticating extrusion process and the liquid conveying process have similar residence time distribution functions. The applicability of some theoretical models for describing the experimental RTD functions for solid and liquid screw conveying and for plasticating extrusion has been shown for each case. The experimental methods with a radioactive tracer which we have described are quite versatile and can be applied to any other unit operation. The potential of the experimental tool is in the possibility of analyzing other types of extruders, like twin screw extruders, poorly performing extruders, the effect of the addition of static mixers, or the effect on the mixing of any other change in the extruder. For example, we are now studying the RTD functions obtained from operating the extruder with various flight clearances. The findings will be reported in a subsequent paper.

ACKNOWLEDGMENT

The authors wish to express their sincere thanks and appreciation to Professors R. L. Seale and G. W. Nelson, and Mr. F. E. Haskin of the Nuclear Engineering Department, University of Arizona, for their advice and help in performing this experimental work.

We also want to thank the InMont Corporation for kindly providing us with the polyester resin and the Dart Industries and Dow Chemical for supplying the low density polyethylenes.

NOTATION

a = normalized height in the channel, natural abundance of active isotope
A_w = correction factor for change in channel depth
C = concentration distribution function, counts/s
$C(t)$ = radioactive activity at time t
$C(o)$ = radioactive activity at time zero
D = barrel diameter
D_e = eddy diffusivity
E = residence time distribution function
F = cumulative residence time distribution function
H = channel depth
h = channel depth after the tapered section
I_A = intensity of activation
L = length of screw of extruder
M = atomic weight, amount of irradiated material
n = number of tanks in series
N = number of mean residence times; Avogadros number
P = pressure, fraction of plug flow
P_1 = pressure at the beginning of the transition section
P_2 = pressure at the beginning of the metering section
P_3 = pressure at the die
Q = flow rate
T = temperature
T_1 = temperature of the melt at the point where P_1 is measured
T_2 = temperature of the melt at the point where P_2 is measured
T_3 = temperature of the melt at the tip of the screw
T_4 = temperature of the melt at the die
T_5 = temperature of outside surface of barrel at rear 1
T_6 = temperature of outside surface of barrel at zone 2
T_7 = temperature of outside surface of barrel at die 1
T_8 = temperature of cooling water for the conveying section of the screw
t = time
$t_{1/2}$ = half-life of produced radioisotope

$\bar{t}$ = mean residence time
$\bar{t}_c$ = mean residence time for an extruder with constant channel depth of screw and time elapsed from end of irradiation
t_i = time of irradiation
$\bar{t}_t$ = mean residence time for tapered channel depth of screw
u = velocity of flow
V = holdup of extruder
V_b = tangential velocity of barrel
V_z = down-channel velocity component of barrel
x = height in the nuclear reactor
W = channel width, weight of irradiated sample

Greek Letters

θ = helix angle, normalized time
ϕ = pressure to drag flow ratio, neutron flux
η = efficiency of flux, coefficient of exponent
ϵ = system phase shift
σ = cross section of isotope to nuclear reaction, cm^{-2}
γ = coefficient for decay, $0.693/t_{1/2}$

LITERATURE CITED

Chase, G. D., and J. L. Rabinowitz, *Principles of Radioisotope Methodology*, 2 ed., Burgess Publishing Comp., Minneapolis, Minn. (1962).

Felix, J., "Analysis of Temperature Profiles in a Screw Cooled Plasticating Extruder," M.Sc. thesis, Univ. Ariz. (in preparation 1975).

Levenspiel, O., *Chemical Reaction Engineering*, 2 ed., Wiley, New York (1972).

Pinto, G., and Z. Tadmor, "Mixing and Residence Time Distribution in Melt Screw Extruders," *Polymer Eng. Sci.*, **10**, 270 (1970).

Pinto, G., "Mixing and Residence Time in a Screw Extruder," M.Sc. thesis, Technion, Haifa, Israel (1969).

Schott, N. R., "Analysis of Plastics Extruder Dynamics," Ph.D. thesis, Univ. Ariz. (1971).

Tadmor, Z., and I. Klein, *Engineering Principles of Plasticating Extruders*, Van Nostrand Reinhold Company, New York (1970).

Tadmor, Z., Private Communication (Feb., 1973).

Todd, D. B., "Mixing in Starved Twin Screw Extruders," Chemical Engineering Progress, **71**, 81, (1975).

Weast, R. C., *Handbook of Chemistry and Physics*, 54 ed., The Chemical Rubber Co., Cleveland, Ohio (1973).

White, D. H., and N. R. Schott, "Dynamics Testing of Plastics Extrusion System," SPE ANTEC, 797 (1971).

Wolf, D., and W. Resnick, "Residence Time Distribution in Real Systems," *Ind. Eng. Chem. Fundamentals*, **2**, 287 (1963).

Zinlichem, D. J. V., J. G. de Swart, and G. Buisman, "Residence Time Distribution in an Extruder," *Lebensm.-Wiss. V. Technol.*, **6**, 184 (1973).

Manuscript received December 3, 1974; revision received October 15, and accepted October 17, 1975.

Secondary Nucleation of Ice in Sugar Solutions and Fruit Juices

From thermal response measurements, ice nucleation rates in distilled water, sugar solutions, and fruit juices were determined for a stirred, batch-seeded crystallizer. High resolution thermometry permitted use of initial subcoolings between 0.01° and 0.2°K. Nucleation increased with approximately the second power of subcooling. Applications to freeze concentration are considered.

JAMES H. STOCKING
and
C. JUDSON KING

Department of Chemical Engineering
University of California
Berkeley, California 94720

SCOPE

The development of freeze concentration processes for food liquids has been hampered by the tendency for very fine ice crystals to form and for the separation of residual concentrate from the ice crystals to be difficult as a result. Incomplete separation of entrained concentrate from the ice results in substantial washing requirements and/or loss of valuable food product.

The size distribution of ice crystals formed during freeze concentration should depend upon the nature and interactions of the nucleation and crystal growth phenomena taking place in the crystallizer. Fundamental, quantitative understanding of these phenomena is then required for rational analysis, design, and improvement of freeze concentration processes.

In this work, the kinetics of ice nucleation were inferred from high resolution measurement of the initial thermal response of a batch crystallizer, following seeding. Quartz thermometry was used so that a range of initial subcooling from 10 to 200 mK could be covered. Studies were performed with distilled water, solutions of sucrose and fructose, apple juice, and orange juice. Interpretation was accomplished through an equation describing the initial thermal response. By comparison with experimental measurement of the initial response, the applicability of this equation could be evaluated, and the nucleation parameters could be inferred from the experimental response.